energies

MDPI

Article

Feasibility Study of the Solar-Promoted Photoreduction of CO_2 to Liquid Fuels with Direct or Indirect Use of Renewable Energy Sources

Francesco Conte [1], Antonio Tripodi [1], Ilenia Rossetti [1] and Gianguido Ramis [2,*]

[1] Chemical Plants and Industrial Chemistry Group, Dip. Chimica, Università degli Studi di Milano, CNR-SCITEC and INSTM Unit Milano-Università, via C. Golgi 19, 20133 Milan, Italy; francesco.conte@unimi.it (F.C.); antonio.tripodi@unimi.it (A.T.); ilenia.rossetti@unimi.it (I.R.)

[2] Dip. Ing. Chimica, Civile ed Ambientale, Università degli Studi di Genova and INSTM Unit Genova, via all'Opera Pia 15A, 16145 Genoa, Italy; gianguidoramis@unige.it

* Correspondence: gianguidoramis@unige.it

Abstract: Solar irradiation data collected at the latitude of Milan city, near the 45th parallel North, and original activity data of some high-performing photocatalysts (i.e., commercial TiO_2 P25, TiO_2 prepared by flame spray pyrolysis, 0.2% wt/wt Au/P25) have been used to evaluate the feasibility and the efficiency of an ideal solar photoreactor for the CO_2 photoreduction in liquid phase. The best theoretical performance was achieved with commercial bare P25 titania, despite the fact that it was the material with the widest band gap (3.41 eV vs. 3.31 for FSP and 3.12 for Au/P25). In that case the efficiency of energy storage was calculated as about 2% (considering the total irradiated solar energy) and ca 18% (considering only the UV fraction of solar irradiance). Most of the energy content of the products was stored as formic acid, which would return a productivity of about 640 kg/year kg_{cat} under daylight solar irradiation considering the variance of the irradiance data. Bare FSP titania gave a less promising result, while Au/P25 ranked in the middle. A comparison between the proposed setup and a photoreactor irradiated with UV lamps powered through a wind turbine or solar panels, which allow for an indirect use of renewable energy sources also intended for energy storage purposes, unveil that the latter is many times less efficient than the hypothesized direct solar photoreactor, despite the fact that it could be a reasonable storage system for energy production peaks.

Keywords: CO_2 photoreduction; solar energy storage; solar fuels; titanium dioxide; sunlight; photoreactor

Citation: Conte, F.; Tripodi, A.; Rossetti, I.; Ramis, G. Feasibility Study of the Solar-Promoted Photoreduction of CO_2 to Liquid Fuels with Direct or Indirect Use of Renewable Energy Sources. *Energies* **2021**, *14*, 2804. https://doi.org/10.3390/en14102804

Academic Editor: Talal Yusaf and Trong-On Do

Received: 9 March 2021
Accepted: 8 May 2021
Published: 13 May 2021

1. Introduction

It is well known that the amount of energy that reaches the Earth every day as solar radiation largely exceeds the energy demand for human activities [1,2]. Most of the incident radiation belongs to the visible spectrum (i.e., 400–700 nm) and a bare 4%–6% is set in the ultraviolet region, which can be further divided into UVA (320–400 nm), UVB (290–320 nm) and UVC (200–290 nm) [3]. However, almost all the components below 300 nm are absorbed by the ozone layer and are not useful for solar technology exploitation on the Earth's surface [4].

Nowadays, it has been clearly proven that climate change is linked to the massive emission of carbon dioxide into the atmosphere by humankind. CO_2 is mainly released by the energy sector, such as transportation, heat and electricity production, which largely rely on fossil fuels [5]. Indeed, hydrocarbons and coal represent efficient energy vectors due the high energy density (roughly 45.6 MJ/kg for diesel-type fuel and 24 MJ/kg for coal) [6], easy handling and low cost. However, alongside the carbon dioxide emissions

upon their combustion, another main issue is that these resources are limited and are not renewable through natural cycles, at least not on a human time scale.

Despite many efforts to dispose of carbon dioxide in alternative ways, such as Carbon Capture and Sequestration (CCS), one of the most promising approaches to reduce the rate of CO_2 emissions is to convert it into regenerated chemicals [7–10]. As a reagent, carbon dioxide is too stable to react spontaneously under mild conditions (i.e., low temperature and low pressure), but catalyzed reactions and electrochemical processes proved to be effective for the production of methanol, methane, formaldehyde, formic acid and carbon monoxide [11–14]. A further step towards the sustainability of that kind of treatment is the exploitation of a renewable energy source to support the energy demanding up-hill reactions from CO_2 to regenerated fuels [15–20], among which the most fascinating is certainly solar radiation. In particular, electrochemical reduction may take advantage of existing photovoltaic plants, though their theoretical efficiency is capped at 30% in the case of silicon-based panels [21], further lowered by considering the efficiency of electrochemical CO_2 conversion, while it is gaining more popularity in the concept of photocatalyzed processes [22–28]. In the latter case, a semiconductor is employed that harvests light of appropriate wavelength forms in a photoexcited electron-hole couple. The latter is used to promote redox reactions; in this case the photopromoted electron reduces CO_2 to formic acid, formaldehyde, methanol or methane [29].

Many materials have been studied as potential photocatalysts [30]; however, most of them do not find applications outside of research laboratories. Moreover, the design of the photoreactor, as well as the process optimization, are often left in the background, while they are crucial to improve the efficiency and to compete with existing processes. In this work, we propose a feasibility assessment for a plant for the photoreduction of CO_2 to liquid fuels. The results are based on original experimental data [12] collected by means of a homemade high-pressure photoreactor in which the process was carried out using pure titania and gold-loaded titania photocatalysts. Since the reactor is made of steel and presents a significant capacity (about 1.5 L) with respect to most literature reports (mainly dealing with few mL) it may be a good benchmark for scale-up [14,31–34]. We here collected real-time data of solar irradiance that allowed us to calculate the expected productivity of our photocatalysts in case sunlight should be employed as a photon source to perform the reaction with direct solar energy absorption.

Furthermore, the theoretical productivity achieved with the direct exploitation of the sunlight is compared with the performance that would be reached if the photoreactor would employ electrical energy obtained from renewable sources. Indeed, the photoreactor may be differently designed (a) for direct irradiance by solar light or (b) for use with UVA lamps that may be feed with renewable electricity. In option (b) photovoltaic (PV) panels and wind turbines are explored as sources of electricity for the lamps that irradiate the photoreactor. A scheme of both the proposed setups is reported in Figure 1.

To sum up, besides huge efforts in designing attractive materials for the photoreduction of CO_2, little effort has been devoted to understanding the real feasibility of the process and in the identification of the bottlenecks. Therefore, in this work, starting from some of the most promising results for this reaction, we analyse the possible exploitation of the process under sunlight, calculating major products yield and the amount of stored solar energy, proposing an efficiency factor that benchmarks the applicability of the technology.

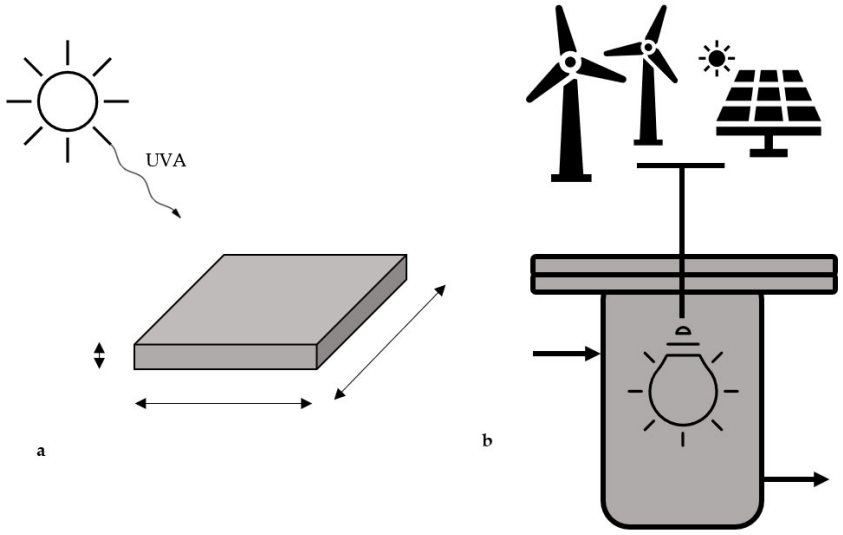

Figure 1. Scheme of the proposed photoreactor for the direct solar driven photoreduction of CO_2 (**a**) and representation of the steel reactor powered with energy from renewables (**b**).

2. Experimental

2.1. Photocatalysts

P25 is a commercial titania supplied by Evonik [35], prepared by flame decomposition and oxidation of a volatile titanium chloride precursor and widely used as benchmark for photocatalysis.

FSP (Flame Spray Pyrolysis) titania was obtained using a homemade apparatus already described elsewhere [36]. Shortly, the titania precursor solution is obtained by dissolution of titanium isopropoxide (Sigma Aldrich (Milano, Italy), purity 97%) in the proper amount of o-xylene and propionic acid (Sigma Aldrich, purity 97%) with a 0.4 M concentration. Then the solution is pumped at constant rate (2.5 mL/min) through a needle which is fixed in the center of a burner. The spraying nozzle is surrounded by many flamelets fed with a mixture of methane and oxygen (0.5 L/min and 1.0 L/min), while the precursor is dispersed by means of an oxygen co-current flow (5 L/min). The pressure drop at the burner nozzle was set to 1.5 bar. Due to the high temperature, the solution is instantly vaporized and pyrolysis, with the formation of titania nanoparticles that are collected on the wall of a glass bell surrounding the burner.

Then, 0.2% wt/wt Au/P25 was prepared via chemical deposition, described in detail elsewhere [31]. Briefly, the selected amount of P25 titania and urea are added to distilled water, then the solution is heated at 80 °C and a $NaAuCl_4$ aqueous solution is added under vigorous stirring. After several hours, the catalyst was filtered and washed with distilled water, then it was suspended in distilled water and $NaHBH_4$ was added under stirring at room temperature in order to reduce the gold precursor over the titania surface.

The catalysts used were thoroughly characterized as described elsewhere [14].

2.2. Photoreactor

All the photoreduction experiments were carried out in a double wall cylindrical batch-type photoreactor with a net capacity of 1.3 L. The reactor is made of stainless steel (AISI 316) and jacketed, thus the temperature can be managed by recirculation of water. The cap mounts a quartz sleeve in which the UV lamp is located and that allows to work at pressure up to 20 bar. The operation at a pressure higher than the ambient pressure showed that it was pivotal to over-perform literature data. The solution is stirred through a magnetic mixer (400 rpm).

All the tests were performed by addition of the selected amount of photocatalyst (0.031 g/L), hole scavenger (HS, sodium sulfite 1.67 g/L) and distilled water (1.2 L), then the pH was adjusted to 14 by addition of sodium hydroxide tablets (about 11.67 g/L). Once sealed, the reactor was outgassed with a flow of CO_2 until few traces of air were detected through GC analysis, then it was set to the desired operating pressure (6–20 bar) for one night in order to absorb the carbon dioxide into water. The reaction starts when the reactor reaches 80 °C and the UV lamp is switched on.

Irradiation was provided by means of a medium-pressure mercury UVA lamp with two emitting bulbs (250 W, 354 nm), while its irradiance was periodically checked with a photoradiometer (Delta OHM (Caselle di Selvazzano, Padova, Italy) HD2102.2) and resulted to be on average 150 W/m^2.

The evolution of gaseous products (e.g., CO, CH_4, H_2) was estimated via gas chromatography using the proper setup (Agilent (Santa Clara, California, USA), mod. 7890, He as a carrier, TCD detector), whereas liquid compounds were quantified by means of HPLC (Agilent, 1220 Infinity, column Alltech, OA-10308) equipped with UV and refractive index detectors (Agilent, 1260 Infinity). The mobile phase was an aqueous solution of H_3PO_4 (0.1% wt/wt). The residual amount of HS was evaluated via iodometric titration. Briefly, a precise amount of potassium iodate is added to the sample as well as an excess of potassium iodide and hydrochloric acid. Then, the orange mixture is titrated with a standard solution of sodium thiosulfate until full discoloration. All the reagents employed to perform the reaction and the calibration were employed without further purification and were purchased from Sigma Aldrich.

3. Results and Discussion

3.1. Photoreduction of CO_2 in a Direct Solar Photoreactor (Case A)

The target reaction is the photoreduction of CO_2 in water with dispersed titania as a photocatalyst. The main drawback is the poor solubility of CO_2 in the working solvent which has been counterbalanced by increasing both the pH of the solution to pH 14 and the pressure up to 20 bar [14,37]. In general, as pointed out in Figure 2, the photoreduction of CO_2 is a complex process that involves multiple reaction steps in which the reactant, dissolved in water and adsorbed over the photocatalyst surface, reacts with the photoexcited electrons [29]. Overall, the efficiency of the reaction is affected by the tendency of the electron-hole couple to recombine and, moreover, the oxidation reaction of water, which should consume the holes closing the circuit, is kinetically disfavored due to the 4e$^-$ passage required for its completion to a stable product [38].

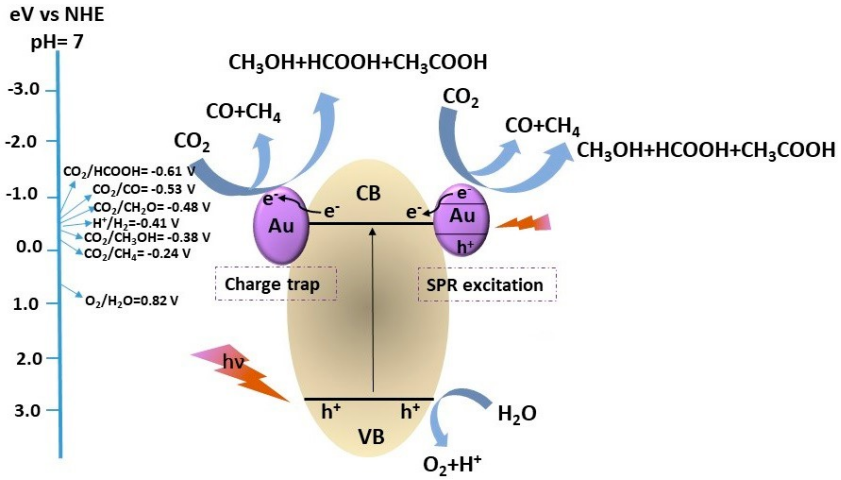

Figure 2. Simplified reaction mechanism of the CO_2 photoreduction over a photocatalyst [14], reproduced with permission from [Bahadori, E.; Tripodi, A.; Villa, A.; Pirola, C.; Prati, L.; Ramis, G.; Rossetti], [Catalysts]; published by [MDPI], 2014].

In order to overcome such limitations, several approaches have been studied; for instance, deposition of a metallic co-catalysts over the titania surface has proven to reduce the rate of charge recombination via the formation of a Schottky barrier, or more in general acting as electron sink [39]. Besides, it is possible to avoid hole accumulation by employing a sacrificial agent, the "hole scavenger" (HS) which is added to the solution. It may be an organic substrate easily oxidizable (e.g., methanol, formic acid, etc.) or an inorganic one (e.g., sodium sulfite), as in the present case [14]. As long as there is enough HS in the solution, the reaction proceeds with appreciable rates and CO_2 is converted into liquid phase products: HCOOH was the main product in the basic medium, accompanied by HCHO and CH_3OH in neutral conditions [40], but the latter was with much lower productivity. These compounds can act as HS themselves when there are no other easily oxidizable compounds into the solutions, for instance when the original HS has been fully consumed [32]. Therefore, the consumption of organics as HS favors the release of gaseous products such as CO, CO_2, H_2 and even methane, though this fully reduced compound was detected in a few cases only, and with very limited productivity [16].

In the following scheme, all the reasonable products and intermediates are presented.

1. $CO_2 + 2H^+ + 2e^- \rightarrow CO + H_2O$
2. $CO_2 + 2H^+ + 2e^- \rightarrow HCOOH$
3. $CO_2 + 4H^+ + 4e^- \rightarrow HCHO + H_2O$
4. $CO_2 + 6H^+ + 6e^- \rightarrow CH_3OH + H_2O$
5. $CO_2 + 8\ H^+ + 8e^- \rightarrow CH_4 + 2H_2O$
6. $2H^+ + 2e^- \rightarrow H_2$

Of course, reactions (1) and (2) are the most likely to be carried out, requiring the consumption of a lower amount of electrons, although (3) and (4) may become important depending on reaction conditions. Furthermore, hydrogen evolution (6) is always in competition with CO_2 photoreduction.

Currently, the solution is irradiated in the steel photoreactor with a medium pressure UV lamp, the maximum emission of which is set in the UVA range (365 nm). One of our main goals is to perform the reaction using the most abundant and renewable source of photons, that is the sun [41]. Thus, it is interesting to estimate the performance of a photoreactor possibly exposed to sunlight. In order to do that, we combined activity data collected in our steel reactor with measures of solar irradiance to calculate the possible product productivity and thus estimate the feasibility and efficiency of the process. Of course, only the UVA fraction of the sunlight has been considered, since it is the portion of the UV spectra that can almost freely reach the Earth's surface.

We performed the reaction using the global solar irradiance (i.e., the sum of direct, diffuse and reflected irradiation) at the Milan city (Italy) latitude, which is 45°27′40.68″ North, as an example of continental site, representing a reasonable average between southern and northern countries in Europe. The data were provided by the Regional Environmental Protection Agency (ARPA) of Lombardy Region, Italy [42].

First of all, it was calculated how much of the measured irradiance was the UV component, about 6% for UVA. The results are reported in Table 1, where only the mean irradiance per month is reported for brevity. Moreover, it was supposed that the radiation was equally distributed along the daytime, giving rise to the overall daily irradiance reported in Table 1.

Table 1. Mean daily irradiance data, classified per month, measured by ARPA during 2018 for the city of Milan, Italy. Last two columns: total energy and UV energy monthly impinging on each m^2 of surface.

Period	Mean Irradiance (W/m^2)	UV Fraction (W/m^2)	Monthly Energy (MJ/m^2)	Monthly UV Energy (MJ/m^2)
JAN	53.1	3.2	142.2	8.5
FEB	77.6	4.7	207.8	11.3

MAR	109.0	6.5	291.9	17.5
APR	201.0	12.1	538.4	31.3
MAY	211.0	12.7	565.1	33.9
JUN	295.0	17.7	790.1	45.9
JUL	286.0	17.2	766.0	46.0
AUG	248.0	14.9	664.2	39.9
SEP	195.0	11.7	522.3	30.3
OCT	108.0	6.5	289.3	17.4
NOV	43.5	2.6	116.5	6.8
DEC	57.5	3.5	154.0	9.2

When the UV radiation hits the photocatalyst surface and is absorbed, it causes the excitation of one electron to the conduction band from the valence band, leaving a hole in the latter. However, only radiation of proper energy can be absorbed, depending on the band gap of the material, thus the narrower is this value and the longer is the maximum wavelength of the absorbed radiation, allowing to better exploit the solar spectrum. On the other hand, if the band gap is too narrow, the absolute energy of the valence and conduction bands may not be suitable to perform the redox reaction of interest [29]. Therefore, the wavelength threshold was calculated according to (Equation (1)), based on Diffuse Reflectance UV data (Table 2).

Since the UV radiation that reaches the Earth's surface lies in the 300–400 nm range, but the material absorption edge may be at shorter wavelength than 400 nm, it was estimated how much of the UV available radiation could be really absorbed by each photocatalyst (Equation (2), Figure 3). The results are reported in Table 2.

In particular the Au-loaded sample was characterized by a contribution of plasmon resonance in the visible region (centered at about 550 nm) due to the fine dispersion of Au nanoparticles, 4 ± 1 nm in size [31].

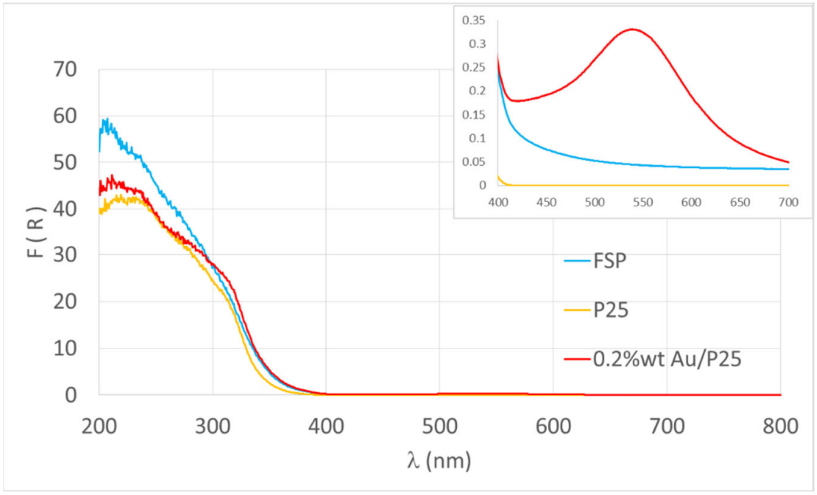

Figure 3. DR-UV spectra of the different samples. Inset: zoom of the visible portion of the spectrum.

$$\lambda_{max}(\text{nm}) = \frac{1240}{\text{BG (eV)}} \quad (1)$$

$$\text{UVA}_{abs} = \frac{\lambda_{max} - 300}{400 - 300} \quad (2)$$

Table 2. Maximum light wavelength that can be absorbed by the listed photocatalysts and percentage of UVA radiation with the required energy to excite the electrons in such materials.

Photocatalyst	BG (eV)	λ_{max} (nm)	% UVA Absorbed
P25	3.41	364	64%
FSP	3.31	375	75%
0.2%wt/wt Au/P25	3.12	397	97%

Since the longer wavelengths are not suitable to perform the reaction, except in the case of Au/P25, which shows the narrower band gap value, absorbing almost all the UV fraction, it is necessary to further correct the value of solar irradiance that were calculated in Table 1 [43]. The UV irradiance was therefore multiplied by the absorbable fraction reported in Table 2, to calculate the useful energy shooting the photocatalyst.

The production rates of the various compounds analyzed in our pilot photoreactor with the UV medium-pressure lamp are summarized in Table 3. As an order of magnitude, the maximum productivity of hydrogen that has been achieved in our high-pressure reactor when using P25 as photocatalyst and a 150 W/m^2 UV irradiance was nearly 4.00 mol_{H2}/h kg_{cat}, for HCOOH was 39.36 mol_{HCOOH}/h kg_{cat} and for CO 0.23 mol_{CO}/h kg_{cat}. In the cases of HCHO and CH_3OH, the production rate was far lower, so they are included in the list but are irrelevant and thus not considered for the subsequent calculation of energy storage efficiency.

Table 3. Production rate values of the relevant products obtained with different photocatalysts (P25, FSP and Au/P25).

Compound	Catalyst	Production Rate (mol/h kg_{cat})	Production Rate (kg/h kg_{cat})
H_2	P25	4.0000	0.0080
	FSP	1.6100	0.0032
	Au/P25	2.0200	0.0040
CO	P25	0.2290	0.0064
	FSP	0.0660	0.0018
	Au/P25	0.5410	0.0151
HCOOH	P25	39.4000	1.8124
	FSP	7.4300	0.3418
	Au/P25	6.9800	0.3211
HCHO	P25	0.0008	0.0000
	FSP	0.0481	0.0014
	Au/P25	0.0148	0.0004
CH_3OH	P25	0.0006	0.0000
	FSP	0.0000	0.0000
	Au/P25	0.0802	0.0026

A tricky point should be discussed when comparing the different catalysts. The effect of co-catalysts addition was checked in references [14] and [31] under the same conditions, highlighting the beneficial effect of Au in small concentration <1 wt%. The ones compared in this feasibility study were the best performing catalyst and conditions. In particular, pH and catalyst concentration (affecting the calculations). The selectivity was different for Au promoted and un-promoted samples: Au increased the selectivity to reforming products (H_2 and CO) consuming more rapidly the HS and, therefore, consuming the liquid products (HCOOH) as hole scavengers themselves. Au is indeed more active as a photocatalyst, but this higher activity promotes consecutive reactions that convert the here desired product. The P25 and Au-loaded P25 samples should be tested either at different HS concentration or at different time (with similar HS conversion) to assess the

specific effect of consecutive reactions, but we have not done this in order to avoid a spurious comparison. The meaning of this comparison is to identify highly productive options for a preliminary feasibility assessment under the same operating conditions.

Each experiment in the photoreactor lasted 5 h and was carried out with an UVA irradiance of 150 W/m^2, with maximum wavelength of 365 nm, fully absorbed by all the catalysts. According to these data, during an experiment the energy supplied by the lamp amounts to 2.7 MJ/m^2 (Equation (3)). Thus, Table 4 reports the amount of products expected (productivity) normalized per mass of catalyst and per MJ/m^2 of incident light (Equation (4)).

Furthermore, based on the average daily irradiance reported in Table 1, corrected by the absorbable fraction, we calculated the total solar energy in one year (MJ/m^2), useful to carry out the reaction over each catalyst (i.e., the UV irradiance only in one year multiplied by the fraction absorbed by each catalyst based on the band gap, as in Table 2) and multiplying such value for the productivity, we calculated the yearly expected productivity for each kg of catalyst (Table 4, last column, Equation (6)).

$$Total\ Incident\ Energy\ \left(\frac{\mathrm{MJ}}{\mathrm{m^2}}\right) = Lamp\ irradiance\ \left(\frac{\mathrm{J}}{\mathrm{s\ m^2}}\right) Testing\ time\ (\mathrm{s}) \quad (3)$$

$$Productivity\ \left(\frac{\mathrm{kg\ m^2}}{\mathrm{MJ\ kg_{cat}}}\right) = \frac{Production\ rate\ \left(\frac{\mathrm{kg}}{\mathrm{h\ kg_{cat}}}\right) Testing\ time\ (\mathrm{h})}{Total\ Incident\ Energy\ \left(\frac{\mathrm{MJ}}{\mathrm{m^2}}\right)} \quad (4)$$

$$Yearly\ useful\ inc.energy\ \left(\frac{\mathrm{MJ}}{\mathrm{m^2}}\right) = Solar\ irradiance\ \left(\frac{\mathrm{J}}{\mathrm{s\ m^2}}\right) 1\ year\ (\mathrm{s})\ Abs.fraction \quad (5)$$

$$Yearly\ productivity\ \left(\frac{\mathrm{kg}}{\mathrm{kg_{cat}}}\right) = Productivity\ \left(\frac{\mathrm{kg\ m^2}}{\mathrm{MJ\ kg_{cat}}}\right) Yearly\ useful\ inc.energy\ \left(\frac{\mathrm{MJ}}{\mathrm{m^2}}\right) \quad (6)$$

Table 4. Normalized productivity of different products, for different catalysts, normalized per kg of catalyst and per MJ/m^2 of incident energy. Yearly productivity expected based on solar irradiance corrected by the fraction of energy absorbed by each catalyst.

Compound	Catalyst	Productivity (kg m^2/MJ kg$_{cat}$)	Yearly Productivity (kg/kg$_{cat}$)
H_2	P25	0.015	2.82
	FSP	0.0060	1.33
	Au/P25	0.0075	2.16
CO	P25	0.012	2.26
	FSP	0.0034	0.76
	Au/P25	0.028	8.1
HCOOH	P25	3.36	639.8
	FSP	0.63	141.4
	Au/P25	0.59	171.8
HCHO	P25	0.00004	0.008
	FSP	0.0027	0.60
	Au/P25	0.00082	0.24
CH_3OH	P25	0.00004	0.007
	FSP	0.00000	0.000
	Au/P25	0.0048	1.37

Considering the calculated values, as expected by the products distribution the only interesting product to be recovered is HCOOH, for which in one year about 640 kg are expected per 1 kg of catalyst. This result is even more interesting since it is obtained with a commercial catalyst with limited absorbance in the visible part of the spectrum, leaving

ample room for the design of visible sensitive catalysts, which should significantly enhance the productivity of this compound. Furthermore, with the other products being negligible, the operating conditions may be finely tuned to further optimize the photoconversion of CO_2 to formic acid.

At this point, it is even more useful to consider the Energy Storage Capacity (ESC) of the process in the chemical compounds rather than the productivity of the latter (Equation (7)), to calculate the efficiency of solar light exploitation. Moreover, the conversion is made either for the lower (LHV) and upper (HHV) heating value of the product. The heating values that were found in literature for hydrogen are, respectively, 120 and 142 MJ/kg [44]. In addition, the entire efficiency of the process can be seen as the total amount of energy stored into the chemical bonds of the products with respect to the energy delivered by the sunlight, either considering the whole irradiance and the useful fraction only (Tables 1 and 2, respectively). To do this, reasonable hypotheses on the reactor geometry should be established, to suppose an irradiated surface and to calculate the total energy impinging on the catalyst.

Hence, a solar photoreactor was considered, holding 1 kg of catalyst in the same concentration of the pilot scale experiments (31 g/m^3, so 32 m^3 reactor). This is a very low concentration, but it is in line with the expected mass per unit volume or surface of supported catalysts, that should be set up for the future exploitation of the system, so it is taken as a conservative datum.

In order to allow uniform light penetration into the suspension, a maximum depth of 0.5 m was considered, which would represent an exposed surface of 64 m^2. According to the solar irradiance of Table 1, during 1 year a total energy of 325.7 GJ would hit such photoreactor surface and the yearly amount of UV light would be accordingly 19.2 GJ. From these data it is possible to calculate the efficiency (η) of the process, either based on the total impinging energy and on the UV fraction, only (Equation (8)) [45]. The catalyst concentration was kept equal to the experimental tests, i.e., 0.031 kg/m^3, and the results are summarized in Table 5.

$$ESC\ (from\ LHV\ or\ HHV)\left(\frac{\mathrm{MJ}}{\mathrm{kg_{cat}}}\right) = Yearly\ productivity\left(\frac{\mathrm{kg}}{\mathrm{kg_{cat}}}\right) LHV\ (or\ HHV)\left(\frac{\mathrm{MJ}}{\mathrm{kg}}\right) \quad (7)$$

$$\eta\ (total\ or\ UV)\% = \frac{ESC\ (from\ LHV\ or\ HHV)\left(\frac{\mathrm{MJ}}{\mathrm{kg_{cat}}}\right)\ 1\ (\mathrm{kg_{cat}})}{Yearly\ total\ solar\ (or\ UV) energy\left(\frac{\mathrm{MJ}}{\mathrm{m^2}}\right)\ Surface\ solar\ reactor\ (\mathrm{m^2})} \times 100 \quad (8)$$

Table 5. Energy Storage Capacity that can be potentially stored in HCOOH and in H_2, i.e., the main products, through the photoreduction of CO_2 and efficiency calculated based on total and UV solar radiation. Data referred to catalyst P25.

		Total Solar Energy			
ESC_{H2} LHV (MJ/kg$_{cat}$)	**ESC_{H2} HHV (MJ/kg$_{cat}$)**	**η_{H2} LHV**	**η_{H2} HHV**	**ESC_{HCOOH} (MJ/kg$_{cat}$)**	**η_{HCOOH}**
338.6	400.6	0.10%	0.12%	3519	1.1%
		UV solar energy			
		1.76%	2.08%		18.3%

It evident that the efficiency of the energy storage is very low, even considering the P25 catalyst and the production of HCOOH. The efficiency of exploiting the UV portion of solar energy is reasonable, though it leaves room for the optimization of the catalyst properties to increase the productivity. The key point, however, is to improve the exploitation of the widest portion of the solar radiation spectrum, currently used for 2% only.

To date, this type of treatment does not have the potential to compete with any commercial process for solar energy conversion, since in case of inexpensive domestic

photovoltaic systems the overall efficiency is close to 20%, i.e., one order of magnitude higher [46].

However, the key point of this evaluation is to assess whether it would be feasible to perform the photoreduction of CO_2, which is a waste molecule, under sunlight and with production of regenerated fuels. Moreover, it is likely that a photoreactor built at latitude closer to Equator would perform much better in terms of productivity (though not affecting efficiency) since the yearly irradiance is almost double with respect to the central Europe, so improving even more the productivity of this chemical [45].

In other words, CO_2 photoreduction through sunlight may replace the current CCS technique due to the high cost of the latter, which vary between the 24 and 47 USD/tCO_2 just for the separation, while it has to be added to the cost for compression (10–13 USD/tCO_2) and transportation (extremely dependent on site location) [10]. In addition, it has been reported that a typical CCS facility installed in series to an energy production plant consumes about 0.8 MW/day when the rated capacity is 40 tCO_2/day [9], thus it is clear that CCS cannot be a long term solution to prevent the annual CO_2 emission, which amounted to about 30 Gton in 2014 [47]. Thus, even if the stage of development of CO_2 photoreduction is too immature for a complete and reliable business model, it is clear that a cost effective and efficient valorization of CO_2 into regenerated fuels or chemicals is compulsory to sustain the virtuous pathway towards a reduction of carbon emissions.

3.2. Indirect Exploitation of Electric Energy from Renewable Sources

The efficiency of the photoreduction process directly exploiting solar energy, as in the previous section, seems to be low for practical application. This is not really important for the use of a free energy source, provided that the productivity is sufficiently large to remunerate in due time the investment for the photoreactor. However, when computing the efficiency with respect to the overall irradiance the value is apparently by far lower than more conventional systems for solar light usage, such as Photovoltaic Panels (PV). Therefore, it is possible to consider as an alternative a more efficient way to exploit solar energy to obtain electricity, which is in turn used to sustain an UVA lamp in the photoreactor, indirectly sustained by renewable solar energy. In this sense, CO_2 photoreduction may also represent a way to store electrical energy in case of intermittent renewable energy sources, such as photovoltaic panels and wind turbines. Regarding the former, it is interesting to evaluate how large would be the surface of PV panels required to power every day for one year the 250 W lamp inserted in the photoreactor. In general, commercial photovoltaic panels reach a 20% efficiency in converting the energy from solar radiation into electrical energy and if we consider that the average yearly irradiation at the latitude of Milan results to be 1.38 MWh/m^2 it is possible to calculate the panels surface required to meet the energy consumption required to feed the lamp (Equation 9). One-year continuous operation of the 250 W lamp would require 7.9 GJ of electric energy supply, assuming 24 h operation. This would lead to the production of 0.6 kg of HCOOH per year, considering the size of the current reactor. However, this cannot be furnished through PV panels, because about 10 h average irradiation per day can be roughly assumed. Therefore, considering to operate the photoreactor for 10 h per day to store solar energy would result in 3.3 m^2 of photovoltaic panels (Equation (10)).

In contrast, considering this assembly not for the purpose of PV solar energy storage but for the primary goal of a continuous process for the photoconversion of CO_2, given the alternating between day and night, a different storage media for electrical energy (e.g., a battery) would be needed, to sustain the process during nighttime or insufficient radiation. Neglecting in this moment the efficiency of this supplementary energy storage device and considering only the PV panels surface needed to supply the full 24 h electricity needs of the photoreactor, this area would be about 8 m^2. However, this solution would require the capital cost of the photoreactor (more compact), of the PV panel and of the energy accumulation system. Overall, to reach the same productivity of the solar photoreactor, a much higher surface of PV panels would be required.

A different renewable energy conversion system, widely spread and commercialized all over the world are wind turbines. Wind energy suffers of the same problems of intermittency and poor stability, except in selected areas off-shore, and needs accumulation systems in form of batteries or coupling with the synthesis of a proper energy vector. The possibility to couple the here presented CO_2 photoreactor device with a wind turbine is thus explored in the following, to assess if higher feasibility may be reached than for PV panels.

The coupling with a storage system is different in the case of wind turbines, since the maximum productivity may be set during the night when the power consumption is minimum. Similar to what was done with the PV system, one can imagine powering the UVA lamp in the photoreactor exclusively with the energy produced by a wind turbine. According to the data provided by the Italian Ministry of Economy and Finance [48], a turbine installed below 25 m (a.t.l.) could produce 500 Wh for every W of rated power, on average in a year. To feed the photoreactor with a 250 W UVA lamp, the turbine can be correctly sized according to (Equations (9) and (11)).

$$Yearly\ power\ consumption\ \left(\frac{\mathrm{MJ}}{\mathrm{year}}\right) = Lamp\ power\ (\mathrm{W})\ time\left(\frac{\mathrm{s}}{\mathrm{year}}\right) \quad (9)$$

$$Panels\ surface\ (\mathrm{m^2}) = \frac{Yearly\ power\ consumption\ \left(\frac{\mathrm{MJ}}{\mathrm{year}}\right)}{Yearly\ irradiation\ \left(\frac{\mathrm{MJ}}{\mathrm{m^2\ year}}\right)\ \mathrm{x}\ Efficiency} \quad (10)$$

$$Turbine\ rated\ power\ (\mathrm{W}) = \frac{Yearly\ power\ consumption\ (\mathrm{MJ})}{Yearly\ power\ production\left(\frac{\mathrm{MJ}}{\mathrm{W}}\right)} \quad (11)$$

The results illustrate that it would be necessary to install a wind turbine similar to the ones adopted in residential size plants, giving rise to about 4.4 kW power.

In these last solutions, the photoreactor can store the energy into feedstocks during peaks of production or periods with less demand and then the chemicals can be used directly as fuels in order to supply energy when needed. Moreover, in an ideal cycle the CO_2 from combustion would be injected again into the photoreactor, so there would not be a net emission into the atmosphere.

4. Conclusions

In this work, it was demonstrated that the photoreduction of CO_2 in liquid phase and at high pressure can be carried out uniquely using the sunlight as a photon source. In addition, the amount of energy converted and stored in the products depends on the photocatalyst employed and the type of compounds formed, as in case of P25 it may theoretically achieve an 18% conversion efficiency, and based on UV irradiance slightly more than 1% considering the total sunlight irradiated. Moreover, P25 gave the best result despite its wider band gap, but generally speaking all the selected photocatalysts were active in formic acid production, with a maximum of 640 kg per kg_{cat} over one year. The energy conversion efficiency of this system is lower than commercial photovoltaic plants and much higher productivities (and remuneration) are expected at latitudes where the daily irradiation is higher than the one of the city of Milan and more constant during the year. Furthermore, there is ample room for improvement in light harvesting of the semiconductor, to further boost productivity and efficiency.

The hypothesized productivity can be achieved by using about 64 m^2 photoreactor, calculated by keeping constant the parameters currently used for testing.

On the other hand, at this stage of the research it seems inconvenient to power the photoreactor lamp directly with energy from renewables, at least in the case of PV panels. Anyway, this configuration theoretically allows us to better comply with the fluctuation of both the production and energy demand, as the excess production would be converted into stable chemicals.

Overall, there is room for the improvement of the overall efficiency both in material formulation and in extending the absorption window of the semiconductor. Overall interesting productivity can be achieved, that can be further boosted by a more effective light utilization and by selecting a high irradiance location.

Author Contributions: Conceptualization, I. Rossetti. and G. Ramis.; methodology, F. Conte.; software, A. Tripodi.; validation, F. Conte, A. Tripodi, I. Rossetti and G. Ramis; formal analysis, A. Tripodi.; investigation, F. Conte; resources, F. Conte; data curation, F. Conte; writing—original draft preparation, F. Conte; writing—review and editing, I. Rossetti; visualization, I. Rossetti.; supervision, G. Ramis; project administration, G. Ramis. All authors have read and agreed to the published version of the manuscript.

Funding: This research received no external funding.

Institutional Review Board Statement: Not applicable.

Informed Consent Statement: Not applicable.

Data Availability Statement: All the data relative to this research are reported in this manuscript.

Conflicts of Interest: The authors declare no conflict of interest.

References

1. Energy Information Administration Office of Integrated Analysis and Forecasting U.S. Department of Energy. *International Energy Outlook*; Energy Information Administration Office of Integrated Analysis and Forecasting U.S. Department of Energy: Washington, DC, USA, 2005.
2. Kabir, E.; Kumar, P.; Kumar, S.; Adelodun, A.A.; Kim, K.H. Solar energy: Potential and future prospects. *Renew. Sustain. Energy Rev.* **2018**, doi:10.1016/j.rser.2017.09.094.
3. Diffey, B.L. Solar Ultraviolet Radiation Effects on Biological Systems. *Phys. Med. Biol.* **1991**, *36*, 299.
4. Fioletov, V.E.; Bodeker, G.E.; Miller, A.J.; McPeters, R.D.; Stolarski, R. Global and zonal total ozone variations estimated from ground-based and satellite measurements: 1964-2000. *J. Geophys. Res. Atmos.* **2002**, *107*, 2615–2621, doi:10.1029/2001JD001350.
5. Lincoln, S.F. Fossil Fuels in the 21st Century. *Ambio* **2005**, *34*, 621–627.
6. Turns, S.R. *An Introduction to Combustion: Concepts and Applications*; McGraw-Hill Higher Education (New York, New York, USA): 2000; ISBN 0-07-230096-5.
7. Olajire, A.A. Valorization of greenhouse carbon dioxide emissions into value-added products by catalytic processes. *J. CO_2 Util.* **2013**, *3–4*, 74–92, doi:10.1016/j.jcou.2013.10.004.
8. Lee, S.Y.; Lee, J.U.; Lee, I.B.; Han, J. Design under uncertainty of carbon capture and storage infrastructure considering cost, environmental impact, and preference on risk. *Appl. Energy* **2017**, doi:10.1016/j.apenergy.2016.12.066.
9. Lee, B.J.; Lee, J.I.; Yun, S.Y.; Lim, C.S.; Park, Y.K. Economic evaluation of carbon capture and utilization applying the technology of mineral carbonation at coal-fired power plant. *Sustainability* **2020**, *12*, 6175, doi:10.3390/su12156175.
10. Pilorgé, H.; McQueen, N.; Maynard, D.; Psarras, P.; He, J.; Rufael, T.; Wilcox, J. Cost Analysis of Carbon Capture and Sequestration of Process Emissions from the U.S. Industrial Sector. *Environ. Sci. Technol.* **2020**, *54*, 7524–7532, doi:10.1021/acs.est.9b07930.
11. Indrakanti, V.P.; Kubicki, J.D.; Schobert, H.H. Photoinduced activation of CO2 on Ti-based heterogeneous catalysts: Current state, chemical physics-based insights and outlook. *Energy Environ. Sci.* **2009**, *2*, 745–758, doi:10.1039/b822176f.
12. Liu, L.; Li, Y. Understanding the reaction mechanism of photocatalytic reduction of CO_2 with H_2O on TiO_2-based photocatalysts: A review. *Aerosol Air Qual. Res.* **2014**, *14*, 453–469, doi:10.4209/aaqr.2013.06.0186.
13. Schneider, J.; Matsuoka, M.; Takeuchi, M.; Zhang, J.; Horiuchi, Y.; Anpo, M.; Bahnemann, D.W. Understanding TiO_2 Photocatalysis: Mechanisms and Materials. *Chem. Rev.* **2014**, *114*, 9919–9986, doi:10.1021/cr5001892.
14. Bahadori, E.; Tripodi, A.; Villa, A.; Pirola, C.; Prati, L.; Ramis, G.; Rossetti, I. High pressure photoreduction of CO2: Effect of catalyst formulation, hole scavenger addition and operating conditions. *Catalysts* **2018**, *8*, 430, doi:10.3390/catal8100430.
15. Kim, J.; Kwon, E.E. Photoconversion of carbon dioxide into fuels using semiconductors. *J. CO_2 Util.* **2019**, *33*, 72–82, doi:10.1016/j.jcou.2019.05.012.
16. Ulmer, U.; Dingle, T.; Duchesne, P.N.; Morris, R.H.; Tavasoli, A.; Wood, T.; Ozin, G.A. Fundamentals and applications of photocatalytic CO_2 methanation. *Nat. Commun.* 2019, *10*, doi:10.1038/s41467-019-10996-2.
17. Murcia Valderrama, M.A.; van Putten, R.-J.; Gruter, G.-J.M. The potential of oxalic-and glycolic acid based polyesters (review). Towards CO_2 as a feedstock (Carbon Capture and Utilization-CCU). *Eur. Polym. J.* **2019**, *119*, 445–468, doi:10.1016/j.eurpolymj.2019.07.036.
18. Wang, C.; Sun, Z.; Zheng, Y.; Hu, Y.H. Recent Progress in Visible Light Photocatalytic Conversion of Carbon Dioxide. *J. Mater. Chem. A* **2019**, *7*, 865–887, doi:10.1039/C8TA09865D.

19. Pomilla, F.R.; Brunetti, A.; Marcì, G.; GarcÍa-López, E.I.; Fontananova, E.; Palmisano, L.; Barbieri, G. CO2 to Liquid Fuels: Photocatalytic Conversion in a Continuous Membrane Reactor. *ACS Sustain. Chem. Eng.* **2018**, *6*, 8743–8753, doi:10.1021/acssuschemeng.8b01073.
20. Rafiee, A.; Rajab Khalilpour, K.; Milani, D.; Panahi, M. Trends in CO_2 conversion and utilization: A review from process systems perspective. *J. Environ. Chem. Eng.* **2018**, *6*, 5771–5794, doi:10.1016/j.jece.2018.08.065.
21. Richter, A.; Hermle, M.; Glunz, S.W. Reassessment of the limiting efficiency for crystalline silicon solar cells. *IEEE J. Photovoltaics* **2013**, *3*, 1184–1191, doi:10.1109/JPHOTOV.2013.2270351.
22. Chaudhery Mustansar, H.; Ajay Kumar, M. *Handbook of Smart Photocatalytic Materials*; Elsevier (Amsterdam, Netherlands): 2020; ISBN 9780128190517.
23. Wang, P.; Yin, G.; Bi, Q.; Huang, X.; Du, X.; Zhao, W.; Huang, F. Efficient Photocatalytic Reduction of CO_2 Using Carbon-Doped Amorphous Titanium Oxide. *ChemCatChem* **2018**, *10*, 3854–3861, doi:10.1002/cctc.201800476.
24. Meng, A.; Wu, S.; Cheng, B.; Yu, J.; Xu, J. Hierarchical TiO2/Ni(OH)2composite fibers with enhanced photocatalytic CO2reduction performance. *J. Mater. Chem. A* **2018**, *6*, 4729–4736, doi:10.1039/c7ta10073f.
25. Wei, L.; Yu, C.; Zhang, Q.; Liu, H.; Wang, Y. TiO_2-based heterojunction photocatalysts for photocatalytic reduction of CO_2 into solar fuels. *J. Mater. Chem. A* **2018**, 22411–22436, doi:10.1039/C8TA08879A.
26. Zhang, S.; Yin, X.; Zheng, Y. Enhanced photocatalytic reduction of CO2to methanol by ZnO nanoparticles deposited on ZnSe nanosheet. *Chem. Phys. Lett.* **2018**, *693*, 170–175, doi:10.1016/j.cplett.2018.01.018.
27. Wang, W.; Xu, D.; Cheng, B.; Yu, J.; Jiang, C. Hybrid carbon@TiO_2hollow spheres with enhanced photocatalytic CO_2 reduction activity. *J. Mater. Chem. A* **2017**, *5*, 5020–5029, doi:10.1039/c6ta11121a.
28. Gao, S.; Gu, B.; Jiao, X.; Sun, Y.; Zu, X.; Yang, F.; Zhu, W.; Wang, C.; Feng, Z.; Ye, B.; et al. Highly Efficient and Exceptionally Durable CO2Photoreduction to Methanol over Freestanding Defective Single-Unit-Cell Bismuth Vanadate Layers. *J. Am. Chem. Soc.* **2017**, *139*, 3438–3445, doi:10.1021/jacs.6b11263.
29. Zhang, L.; Mohamed, H.H.; Dillert, R.; Bahnemann, D. Kinetics and mechanisms of charge transfer processes in photocatalytic systems: A review. *J. Photochem. Photobiol. C Photochem. Rev.* **2012**, *13*, 263–276, doi:10.1016/j.jphotochemrev.2012.07.002.
30. Mills, A.; Le Hunte, S. An overview of semiconductor photocatalysis. *J. Photochem. Photobiol. A Chem.* **1997**, *108*, 1–35.
31. Bahadori, E.; Tripodi, A.; Villa, A.; Pirola, C.; Prati, L.; Ramis, G.; Dimitratos, N.; Wang, D.; Rossetti, I. High pressure CO_2 photoreduction using Au/TiO_2: Unravelling the effect of co-catalysts and of titania polymorphs. *Catal. Sci. Technol.* **2019**, *9*, 2253–2265, doi:10.1039/c9cy00286c.
32. Galli, F.; Compagnoni, M.; Vitali, D.; Pirola, C.; Bianchi, C.L.; Villa, A.; Prati, L.; Rossetti, I. CO2 photoreduction at high pressure to both gas and liquid products over titanium dioxide. *Appl. Catal. B Environ.* **2017**, *200*, 386–391, doi:10.1016/j.apcatb.2016.07.038.
33. Bahadori, E.; Ramis, G.; Zanardo, D.; Menegazzo, F.; Signoretto, M.; Gazzoli, D.; Pietrogiacomi, D.; Di Michele, A.; Rossetti, I. Photoreforming of glucose over CuO/TiO_2. *Catalysts* **2020**, *10*, doi:10.3390/catal10050477.
34. Ramis, G.; Bahadori, E.; Rossetti, I. Design of efficient photocatalytic processes for the production of hydrogen from biomass derived substrates. *Int. J. H_2 Energy* **2021**, *46*, 12105–12116, doi:10.1016/j.ijhydene.2020.02.192.
35. P25-EVONIK.
36. Chiarello, G.L.; Rossetti, I.; Forni, L. Flame-spray pyrolysis preparation of perovskites for methane catalytic combustion. *J. Catal.* **2005**, *236*, 251–261.
37. Sander, R. Compilation of Henry's law constants (version 4.0) for water as solvent. *Atmos. Chem. Phys.* **2015**, *15*, 4399–4981, doi:10.5194/acp-15-4399-2015.
38. Haimei, L.; Imanishi, A.; Nakato, Y. Mechanisms for photooxidation reactions of water and organic compounds on carbon-doped titanium dioxide, as studied by photocurrent measurements. *J. Phys. Chem. C* **2007**, *111*, 8603–8610, doi:10.1021/jp070771q.
39. Ola, O.; Maroto-Valer, M.M. Review of material design and reactor engineering on TiO_2 photocatalysis for CO_2 reduction. *J. Photochem. Photobiol. C Photochem. Rev.* **2015**, *24*, 16–42, doi:10.1016/j.jphotochemrev.2015.06.001.
40. Schneider, J.T.; Firak, D.S.; Ribeiro, R.R.; Peralta-Zamora, P. Use of scavenger agents in heterogeneous photocatalysis: truths, half-truths, and misinterpretations. *Phys. Chem. Chem. Phys.* **2020**, *22*, 15723–15733, doi:10.1039/d0cp02411b.
41. Boxwell, M. *Solar Electricity Handbook: A Simple, Practical Guide to Solar Energy : how to Design and Install Photovoltaic Solar Electric Systems*; 2012th ed.; Greenstream Publishing: Ryton-on-Dunsmore, 2012; ISBN 1907670181.
42. ARPA Environmental Measurements
43. Yan, H.; Wang, X.; Yao, M.; Yao, X. Band structure design of semiconductors for enhanced photocatalytic activity: The case of TiO2. *Prog. Nat. Sci. Mater. Int.* **2013**, *23*, 402–407, doi:10.1016/j.pnsc.2013.06.002.
44. Available online: https://www.engineeringtoolbox.com/fuels-higher-calorific-values-d_169.html.
45. Rossetti, I.; Bahadori, E.; Tripodi, A.; Villa, A.; Prati, L.; Ramis, G. Conceptual design and feasibility assessment of photoreactors for solar energy storage. *Sol. Energy* **2018**, *172*, 225–231, doi:10.1016/j.solener.2018.02.056.
46. Shockley, W.; Queisser, H.J. Detailed balance limit of efficiency of p-n junction solar cells. *J. Appl. Phys.* **1961**, *32*, 510–519, doi:10.1063/1.1736034.
47. IEA-Energy related CO_2 emissions.
48. Interactive Wind Atlas.